

Computer simulation study of the dynamic properties of liquid Ni using the embedded-atom model

M. M. G. Alemany, C. Rey, and L. J. Gallego

Departamento de Física de la Materia Condensada, Facultad de Física, Universidad de Santiago de Compostela, E-15706 Santiago de Compostela, Spain

(Received 16 May 1997; revised manuscript received 20 March 1998)

Using the Voter and Chen version of the embedded-atom model, we carried out molecular-dynamics simulations to compute both single-particle and collective time-dependent properties of liquid Ni, and thereby calculated its diffusion constant and shear viscosity, for the latter of which experimental values are available. The calculated values of the dynamic and self-dynamic structure factors are generally in reasonable agreement with the results of inelastic-neutron-scattering experiments. The values calculated for the diffusion constant by several different routes are mutually consistent. The values of the shear viscosity obtained by several different methods are all very similar to available experimental values. [S0163-1829(98)02126-2]

I. INTRODUCTION

The embedded-atom model (EAM), originally developed by Daw and Baskes^{1,2} on the basis of Stott and Zaremba's earlier quasiatom approach,³ has been successfully used to calculate a wide variety of bulk and surface properties of metals and alloys (for a review, see Ref. 4). Recently, the EAM has also been used to describe the behavior of free⁵⁻¹¹ and supported¹²⁻¹⁵ metal clusters. In the EAM, the total energy of the metal system is considered as the sum of the energy necessary to embed each atom in the background electron density set up by the neighboring atoms (the "embedding energy") and an energy from two-body interactions.

Several versions of the EAM have been proposed. They differ in the form of the functions involved and in the method used for their parametrization. In previous work we used the Voter and Chen (VC) version of the EAM (Ref. 16) in molecular-dynamics (MD) simulations performed to analyze the structural and dynamical properties of some one- and two-component clusters.^{7,8,11} The VC method differs from other EAM approaches (in particular, from that of Foiles, Baskes, and Daw¹⁷) in (a) the use of a core-core pair interaction with a medium-range attractive contribution, and (b) the use of properties of the diatomic molecule in fitting the embedding function and pair interaction.

The first application of the EAM to liquid metals was by Foiles,¹⁸ who in an MD investigation of the static structure factors of the late transition and noble metals obtained results in good agreement with those of x-ray experiments.¹⁹ More recently, both the static structures and thermodynamics of liquid transition metals have been described using EAM potentials.²⁰⁻²⁵ However, to our knowledge, EAM-based MD calculations of the dynamical behavior of this kind of system have not yet been carried out. Extensive computer simulation studies of the dynamical properties of liquid metals have only been performed for alkali systems using effective interatomic potentials.²⁶⁻³³ MD simulations have also been carried out to describe the dynamical behavior of Lennard-Jones,³⁴⁻⁴¹ hard-core,⁴² and hard-core Yukawa⁴³ fluids.

In this work we carried out a thorough EAM-based simulation of the dynamical behavior of a liquid transition

metal. The EAM we used was the VC version;¹⁶ since this model has proved very useful for describing the properties of a wide variety of metallic materials, including clusters^{6-8,11} and bulk systems,¹⁶ it was expected to allow reliable description of the dynamical properties of liquid transition metals, too. The metal we considered was liquid Ni, for which results of inelastic-neutron-scattering experiments are available.⁴⁴

In this paper, we discuss both single-particle and collective dynamic properties. The single-particle properties determined are the mean-square displacement $\langle \Delta^2 r(t) \rangle$ and two single-particle correlation functions, the velocity autocorrelation function $\Psi(t)$ and the self-intermediate scattering function $F_s(q,t)$; the collective properties studied are the intermediate scattering function $F(q,t)$ and the longitudinal and transverse current correlation functions $C_l(q,t)$ and $C_t(q,t)$. These properties were used to calculate two transport coefficients: the diffusion constant D and the shear viscosity η . There are no experimental values of the diffusion constant with which to compare calculated values, but the values calculated from our results by several independent routes are mutually consistent. Our calculations are also supported by the values of the shear viscosity obtained by several different methods, which are very similar to available experimental values.⁴⁵ Although our primary goal was to investigate the dynamical properties of liquid Ni using the VC EAM version, results on the static structure factor $S(q)$ were also obtained so as to allow comparison with x-ray¹⁹ and neutron⁴⁶ scattering data and with MD predictions for $S(q)$ obtained by other EAM approaches.^{18,23}

The organization of this paper is as follows. In Sec. II we describe the EAM version used in this paper and sketch the computational method employed in our calculations. In Sec. III we present and discuss the results obtained. Finally, in Sec. IV, we summarize our main conclusions.

II. MODEL POTENTIAL AND COMPUTATIONAL PROCEDURE

A. Model potential

In the EAM,^{1,2,16,17} the energy of a metallic system is written as

$$E = \sum_i F_i(\bar{\rho}_i) + \frac{1}{2} \sum_i \sum_{j \neq i} \phi_{ij}(r_{ij}), \quad (1)$$

where $F_i(\bar{\rho}_i)$ is the energy required to embed atom i into the background electron density at site i ($\bar{\rho}_i$), r_{ij} is the distance between atoms i and j , and $\phi_{ij}(r_{ij})$ is the core-core pair interaction between these atoms. The host electron density $\bar{\rho}_i$ is approximated by superimposing contributions by all the atoms surrounding atom i :

$$\bar{\rho}_i = \sum_{j \neq i} \rho_j(r_{ij}), \quad (2)$$

where $\rho_j(r_{ij})$ is the electron density of atom j at the position of the nucleus of atom i . If the atomic density function $\rho(r)$ and the pair interaction $\phi(r)$ are both known, the embedding energy can be uniquely defined by requiring that the energy given by Eq. (1) match the ‘‘universal’’ equation of state proposed by Rose *et al.*,⁴⁷ which gives the cohesive energy of the metal as a function of the lattice constant.

As indicated above, there are several EAM versions, which differ in the form of the functions involved and in the method used for their parametrization. In this work we used the VC version,¹⁶ in which the atomic electron density is given by

$$\rho(r) = r^6 (e^{-\beta r} + 2^9 e^{-2\beta r}), \quad (3)$$

β being an adjustable parameter, and the pairwise interaction is described by the Morse potential:

$$\phi(r) = D_M \{1 - \exp[-\alpha_M(r - R_M)]\}^2 - D_M, \quad (4)$$

where D_M , R_M , and α_M are, respectively, the depth of the potential, the distance to the minimum, and a measure of the curvature at the minimum. The values of D_M , R_M , α_M , β , and the cutoff distance r_{cut} , at which the functions $\phi(r)$ and $\rho(r)$ and their derivatives are forced to go smoothly to zero, were determined by Voter and Chen¹⁶ for Ni by minimizing the root-mean-square deviation between the calculated and experimental values of the three cubic elastic constants and vacancy formation energy of Ni metal and of the bond length and bond energy of the diatomic molecule. It was Voter and Chen’s values of these parameters that were used in this work. The resulting embedding function was approximated by a cubic spline.

B. Computational procedure

We studied liquid Ni in two different states characterized by the temperature T and the number density ρ : $T = 1775$ K, $\rho = 0.0792 \text{ \AA}^{-3}$ and $T = 1875$ K, $\rho = 0.078 \text{ \AA}^{-3}$. The first state, quite near the melting point ($T_m = 1726$ K, Ref. 48), is the same as was investigated by Foiles¹⁸ and by Holzman *et al.*²³ in describing the static structure and thermodynamical properties of liquid Ni by means of MD simulations using different EAM versions from that used in this paper; the second corresponds to the conditions of the neutron-scattering experiments carried out by Johnson *et al.*,^{44,46} $T = 1870 \pm 10$ K. The experiments of Johnson *et al.* yielded data on the static structure factor $S(q)$;⁴⁶ experimental $S(q)$

data for both the states considered in this paper have been obtained by Waseda¹⁹ using x-ray scattering.

Using the VC EAM described above, we performed MD simulations for a system of $N = 500$ atoms in a cubic box with periodic boundary conditions. The cutoff distance computed for Ni by Voter and Chen,¹⁶ $r_{\text{cut}} = 4.7895 \text{ \AA}$, is smaller than the maximum value allowed, at each density, by the periodic boundary conditions (one-half the boxlength): 9.240985 \AA for $\rho = 0.0792 \text{ \AA}^{-3}$, and 9.288134 \AA for $\rho = 0.078 \text{ \AA}^{-3}$. Hence the full contribution of the potential energy was included in the calculations.

The computational procedure was as follows. For each state, a canonical MD simulation was first carried out using the Nosé constant-temperature technique.⁴⁹ The initial configuration was obtained by melting an fcc structure. The equations of motion were solved using a fourth-order Gear predictor-corrector algorithm⁵⁰ with a time step $t_s = 10^{-4}$ ps. The energy of the system was then calculated by averaging over 5×10^3 time steps after an appropriate initial period for equilibration.

Starting now from a configuration with an energy very close to the average value obtained above, microcanonical MD simulations were performed using the velocity Verlet algorithm⁵⁰ with a time step $t'_s = 2 \times 10^{-3}$ ps (microcanonical simulations are better than canonical simulations for studying dynamical properties because of the difficulty of controlling the heat exchange variable in the Nosé method). After an appropriate initial equilibration period, a configuration (i.e., the positions \mathbf{r}_i and velocities \mathbf{v}_i of the particles) was recorded every $\Delta t = 0.01$ ps (5 time steps). In order to be able to estimate the statistical uncertainty of the results of these microcanonical simulations, the properties of interest were averaged within each of six successive runs of 25×10^3 time steps (i.e., over the 5×10^3 configurations recorded in every run).

All the properties analyzed in this work were computed using standard expressions.^{50–52} To establish notation, we present the formula used for the static structure factor:⁵¹

$$S(q) = \frac{1}{N} \left\langle \sum_i \sum_j \exp[-i\mathbf{q} \cdot (\mathbf{r}_i - \mathbf{r}_j)] \right\rangle, \quad (5)$$

where \mathbf{q} is a wave vector compatible with the periodic boundary conditions [i.e., $\mathbf{q} = (2\pi/L)(n_x, n_y, n_z)$, where L is the length of the simulation box and the n_α are integers] and the angular brackets denote averaging over both the trajectories of the particles (i.e., over the 5×10^3 configurations recorded in every run) and over all the N_q directions corresponding to the same modulus q .

The single-particle dynamics of the system were analyzed by computing the mean-square displacement $\langle \Delta^2 r(t) \rangle$ and the normalized velocity autocorrelation function $\Psi(t)$, which were obtained, in every run, by averaging over time origins separated by 0.05 ps ($5\Delta t$), and the self-intermediate scattering function $F_s(q, t)$, which was calculated by averaging over time origins separated by $5\Delta t$ and over all the N_q directions corresponding to the same modulus q . The collective correlation functions studied here, namely, the interme-

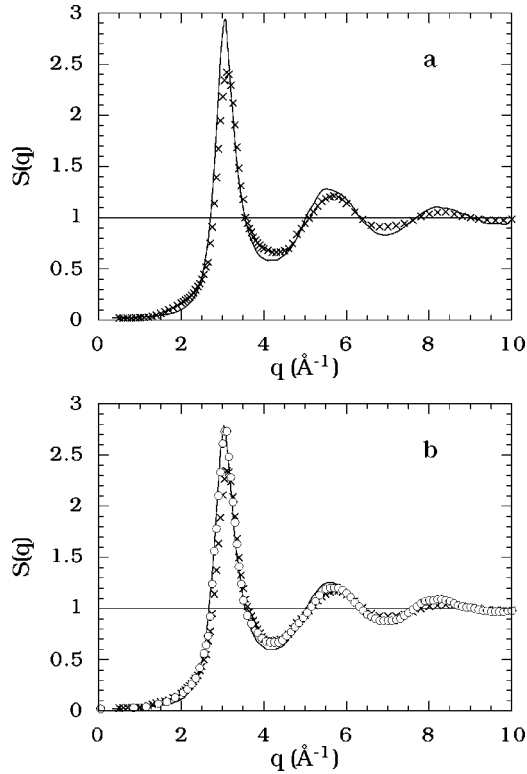


FIG. 1. Static structure factor $S(q)$ for liquid Ni at $T=1775$ K, $\rho=0.0792 \text{ \AA}^{-3}$ [panel (a)] and $T=1875$ K, $\rho=0.078 \text{ \AA}^{-3}$ [panel (b)]. The solid lines represent our EAM MD results, the crosses x-ray-diffraction data (Ref. 19), and the open circles neutron-scattering measurements (Ref. 46).

diate scattering function $F(q,t)$ and the longitudinal and transverse current correlation functions $C_l(q,t)$ and $C_t(q,t)$, were similarly computed using standard relations.⁵¹ The diffusion constant D was calculated from the mean-square displacement using Einstein's formula, and from the normalized velocity autocorrelation function using the Green-Kubo relation.^{50,51} Similarly, the shear viscosity η , a transport coefficient related to collective correlations, was calculated using the Green-Kubo and generalized Einstein formulas.^{31,50}

We also computed the Fourier transforms \mathcal{F} of the correlation functions, i.e., the self-dynamic structure factor $S_s(q,\omega)=\mathcal{F}[F_s(q,t)]$, the dynamic structure factor $S(q,\omega)=\mathcal{F}[F(q,t)]$, $C_l(q,\omega)=\mathcal{F}[C_l(q,t)]$, and $C_t(q,\omega)=\mathcal{F}[C_t(q,t)]$.

III. RESULTS AND DISCUSSION

A. Static properties

In Fig. 1(a) we compare the computed static structure factor $S(q)$ for liquid Ni at $T=1775$ K, $\rho=0.0792 \text{ \AA}^{-3}$ with x-ray data obtained by Waseda¹⁹ for the same thermodynamic state, and in Fig. 1(b) the computed data for $T=1875$ K, $\rho=0.078 \text{ \AA}^{-3}$ are compared with both Waseda's x-ray results¹⁹ and the neutron-scattering results of Johnson *et al.*⁴⁶ for this state. The discrepancy between the x-ray results and simulation [notably in the height of the main $S(q)$ peak] is similar to those obtained for $T=1775$ K, $\rho=0.0792 \text{ \AA}^{-3}$ by Foiles¹⁸ and by Holzman *et al.*²³ in MD

simulations based on different EAM versions from that used here. Holzman *et al.*²³ attributed discrepancy with Waseda's x-ray data to the fact that Ni has a certain degree of directional bonding that is not reflected in the EAM models used. We note, however, that underestimation of the height of the main $S(q)$ peak appears to be a systematic error of the method used by Waseda to analyze his x-ray measurements: for liquid alkali metals, Waseda's value¹⁹ for this parameter is an average 10% lower than that obtained by neutron scattering or other x-ray methods,⁵³⁻⁵⁶ and for Ni in the state $T=1875$ K, $\rho=0.078 \text{ \AA}^{-3}$ there is a difference of the same order with respect to both our computed data and the neutron-scattering results of Johnson *et al.*,⁴⁶ with which our data are in much better agreement [Fig. 1(b)].

B. Single-particle dynamic properties

Figure 2 shows the computed normalized velocity autocorrelation function $\Psi(t)$ of liquid Ni for the states $T=1775$ K, $\rho=0.0792 \text{ \AA}^{-3}$ and $T=1875$ K, $\rho=0.078 \text{ \AA}^{-3}$. The results, which are practically the same for the two states, show the so-called "cage effect,"^{27,28,33} which is characteristic of dense fluids: each atom being enclosed in a small cage formed by the surrounding atoms, it can move over short distances but will then be reflected (causing Ψ to change sign), after which correlation between its instantaneous and initial velocities quickly vanishes. The values of the diffusion constant D obtained using the Green-Kubo and Einstein relations agree well for both the thermodynamic states considered (Table I), and for the state $T=1875$ K, $\rho=0.078 \text{ \AA}^{-3}$ our results also agree quite well with the value $D=0.46 \text{ \AA}^2 \text{ ps}^{-1}$ estimated by Johnson *et al.*⁴⁴ from the results of their neutron-scattering experiments.

For the state closer to the melting point, $T=1775$ K, $\rho=0.0792 \text{ \AA}^{-3}$, the self-intermediate scattering function $F_s(q,t)$ was computed as a function of time for a wide range of wave numbers (Table II). These curves decay monotonically with time for all q values (Fig. 3). For the state $T=1875$ K, $\rho=0.078 \text{ \AA}^{-3}$ we explored 22 q values in the

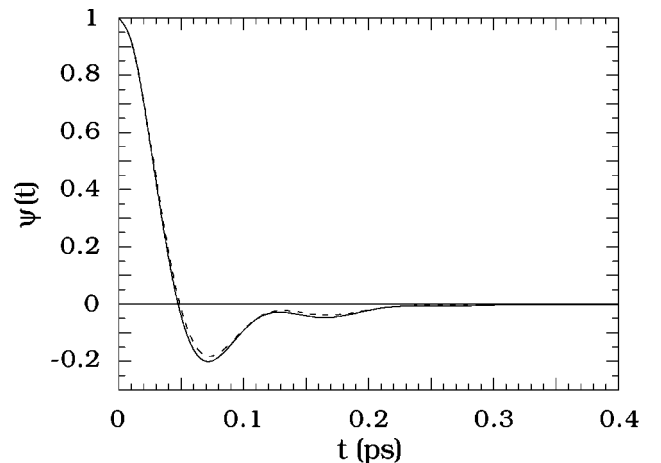


FIG. 2. Normalized velocity autocorrelation function $\Psi(t)$ for liquid Ni as obtained from our EAM MD simulations. The solid line is for the state $T=1775$ K, $\rho=0.0792 \text{ \AA}^{-3}$ and the dashed line for the state $T=1875$ K, $\rho=0.078 \text{ \AA}^{-3}$.

TABLE I. Values of the diffusion constant D (in $\text{\AA}^2 \text{ps}^{-1}$) for liquid Ni at $T=1775$ K, $\rho=0.0792 \text{\AA}^{-3}$ and $T=1875$ K, $\rho=0.078 \text{\AA}^{-3}$, as computed using the Green-Kubo (GK) and Einstein (E) relations. For the state $T=1775$ K, $\rho=0.0792 \text{\AA}^{-3}$, we also show the values obtained by analyzing our MD data in terms of HF, MF, and MC models (see text).

	$T=1775$ K, $\rho=0.0792 \text{\AA}^{-3}$	$T=1875$ K, $\rho=0.078 \text{\AA}^{-3}$
GK	0.352 ± 0.005	0.431 ± 0.004
E	0.356 ± 0.004	0.434 ± 0.004
HF	0.351 ± 0.008	
MF	0.352 ± 0.007	
MC [Eq. (13)]	0.35 ± 0.01	
MC [Eq. (14)]	0.36 ± 0.01	

range $2-5 \text{\AA}^{-1}$, which is close to the range analyzed by Johnson *et al.*⁴⁴ in their neutron-scattering experiments. In Fig. 4 we compare $S_s(q, \omega)$ for this state, as determined from our MD simulations, with the neutron-scattering data reported by Johnson *et al.* for the same constant values of ω .⁵⁷ Except for $\omega=0$ and $q < 3 \text{\AA}^{-1}$ there is fair general agreement between our values and those of Johnson *et al.* In principle, the discrepancy noted could be ascribed to inadequate parametrization of the EAM functions used: as noted in Sec. II A, the embedding function and pair interaction parameters were determined from solid-state data and the properties of the diatomic molecule,¹⁶ which does not guarantee an accurate description of the liquid state. If this is the reason for the discrepancy, it should be possible to improve the EAM description of the liquid state (while still describing the solid accurately) by including liquid-Ni data in the database used for parametrization. However, it seems more probable that the observed discrepancy may be due to the experimental results reported by Johnson *et al.* for $\omega=0$ having rather large errors in the region where the curvature of the $S_s(q, \omega)$ vs q curve is highest: since the data reported by Johnson *et al.* were the result of applying a deconvolution process to their original raw data, any error in the deconvolution function will have led to an error in their reported data that will

TABLE II. Wave numbers q used in the study of the self-intermediate scattering function $F_s(q, t)$ of liquid Ni at $T=1775$ K, $\rho=0.0792 \text{\AA}^{-3}$; the corresponding N_q values are also shown. Except for those marked by an asterisk, the same wave numbers were used in the study of the collective correlation functions.

q (\AA^{-1})	N_q	q (\AA^{-1})	N_q
0.339963	3	1.665472*	12
0.480780	6	1.923121	6
0.588833	4	2.067914*	12
0.679926	3	2.355333	4
0.760180	12	2.719704	3
0.832736	12	3.040721	12
0.961561*	6	3.189136	12
1.127530*	12	3.846243	6
1.225754*	12	4.710667	4
1.359852	3	5.439408	3

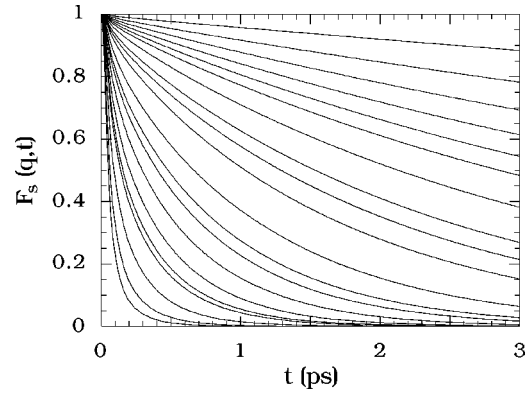


FIG. 3. Self-intermediate scattering function $F_s(q, t)$ for liquid Ni at $T=1775$ K, $\rho=0.0792 \text{\AA}^{-3}$, as obtained from our EAM MD simulations, for the whole q range investigated. From top (smallest q) to bottom (largest q), the wave numbers are those listed in Table II.

be greatest precisely in this region, where the deconvolution correction is largest.⁵⁸ In general, accurate experimental determination of spectral features near $\omega=0$ is a delicate task, and discrepancies between MD and experimental results should not automatically be blamed on the MD calculations. For example, González *et al.*⁵⁹ recently found significant discrepancies between MD $S_s(q, \omega)$ results and experimental data for liquid Li in the region around $\omega=0$, in spite of the potential they used, an interionic pair potential with no adjustable parameters derived from the neutral pseudo-atom method, being capable of very satisfactory reproduction of both the thermodynamic and static structure of liquid Li (over a wide range of temperatures)^{30,31,60} and its dynamical properties (outside the region around $\omega=0$).⁵⁹

Our $F_s(q, t)$ results for the state $T=1775$ K, $\rho=0.0792 \text{\AA}^{-3}$ can be interpreted in terms of hydrodynamic fit (HF), memory function (MF), and mode coupling (MC) models (see Refs. 28, 51, 52, 61, and 62) so as to obtain further values of the diffusion constant D for comparison with those obtained directly from $\langle \Delta^2 r(t) \rangle$ and $\Psi(t)$. Both the HF and MF models for $F_s(q, t)$ contain q -dependent parameters and allow the diffusion constant D to be obtained in the limit $q \rightarrow 0$.

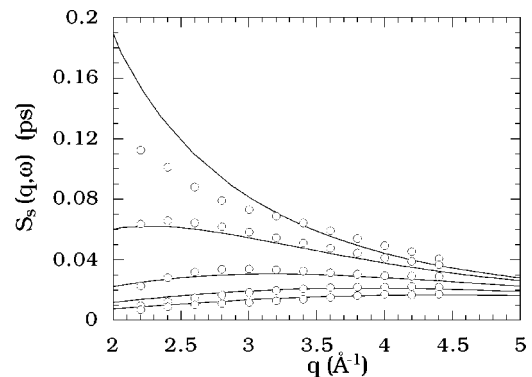


FIG. 4. Self-dynamic structure factor $S_s(q, \omega)$ for liquid Ni at $T=1875$ K, $\rho=0.078 \text{\AA}^{-3}$, for several values of ω (from top to bottom, $\omega=0, 2.28, 4.56, 6.84,$ and 9.12ps^{-1}). The solid lines represent the computed results and the open circles the experimental data (Refs. 44 and 57).

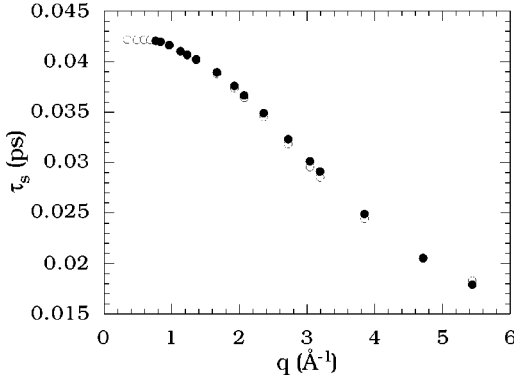


FIG. 5. Relaxation times $\tau_s(q)$ for liquid Ni at $T=1775$ K, $\rho=0.0792 \text{ \AA}^{-3}$. Solid circles represent values obtained by fitting Eq. (9) to our computed $S_s(q, \omega)$ results, open circles values obtained by fitting Eq. (9) to $S_s(q, \omega)$ results computed from Eq. (12) and the values of $D(q)$ obtained from the HF model.

According to the HF model,^{28,51} for small q

$$F_s(q, t) = e^{-Dq^2 t}. \quad (6)$$

The values of the q -dependent generalized diffusion constant $D(q)$ were obtained by fitting Eq. (6) to the MD results of Fig. 3, and extrapolation to $q=0$ gave a value of the diffusion constant D that is in very good agreement with those derived using the Einstein and Green-Kubo equations (Table I).

Our MF model is based on the following ansatz for $N_s(q, t)$, the MF of the MF of $F_s(q, t)$:^{28,51}

$$N_s(q, t) = [2\omega_s^2(q) + \Omega_0^2] e^{-t/\tau_s(q)}, \quad (7)$$

where Ω_0 is the Einstein frequency, $\tau_s(q)$ the relaxation time, and $\omega_s^2(q)$ the second-frequency moment of the self-dynamic structure factor $S_s(q, \omega)$, which is given in terms of the thermal speed v_0 by

$$\omega_s^2(q) = (qv_0)^2 \quad (8)$$

($v_0^2 = kT/m$, where k is the Boltzmann constant and m is the atomic mass). The MF model specified by Eq. (7) yields the expression

$$S_s(q, \omega) = \frac{1}{\pi} \frac{\tau_s(q) \omega_s^2(q) [2\omega_s^2(q) + \Omega_0^2]}{\omega^2 \tau_s^2(q) [\omega^2 - 3\omega_s^2(q) - \Omega_0^2]^2 + [\omega^2 - \omega_s^2(q)]^2}, \quad (9)$$

which to obtain the relaxation times $\tau_s(q)$ plotted in Fig. 5 as solid circles was fitted to $S_s(q, \omega)$ values computed from the $F_s(q, t)$ results of Fig. 3. To fit Eq. (9), the Einstein frequency was calculated from the simulation data using the expression^{50,51}

$$\Omega_0^2 = \frac{\sum_i \langle F_i^2 \rangle}{2m \langle E_k \rangle}, \quad (10)$$

where F_i is the total force exerted on atom i and E_k is the total kinetic energy. In principle, extrapolation of $\tau_s(q)$ to $q=0$ would now allow calculation of the diffusion constant D from the expression^{28,51}

$$\lim_{q \rightarrow 0} \tau_s(q) = \frac{v_0^2}{D\Omega_0^2}. \quad (11)$$

However, since no $S_s(q, \omega)$ values could be calculated for the four smallest q values for which $F_s(q, t)$ was obtained [because $F_s(q, t)$ decayed too slowly to allow computation of its Fourier transform; see Fig. 3], we first computed a second series of $\tau_s(q)$ values (open circles in Fig. 5) by fitting Eq. (9) to $S_s(q, \omega)$ values calculated from our HF values for $D(q)$ using the expression^{28,51}

$$S_s(q, \omega) = \frac{1}{\pi} \frac{D(q)q^2}{[D(q)q^2]^2 + \omega^2}. \quad (12)$$

The two sets of $\tau_s(q)$ values agree well, especially (as is to be expected) for small q , and extrapolation to $q=0$ yielded the value $0.352 \pm 0.007 \text{ \AA}^2 \text{ ps}^{-1}$ for the diffusion constant D , in good agreement with those obtained previously (Table I).

The MC theory of Schepper and Ernst^{61,62} predicts linear q dependence of $S_s(q, 0)q^2$ and $\omega_{1/2}(q)/q^2$, $\omega_{1/2}(q)$ being the half width of $S_s(q, \omega)$ at half maximum:

$$S_s(q, 0)q^2 = \frac{1}{\pi D} (1 + aq), \quad (13)$$

$$\frac{\omega_{1/2}(q)}{q^2} = D(1 - bq), \quad (14)$$

where a and b are parameters that can be determined theoretically from basic quantities and from the diffusion constant and shear viscosity. The values of the diffusion constant D obtained by fitting Eqs. (13) and (14) to values of $S_s(q, 0)q^2$ and $\omega_{1/2}(q)/q^2$ calculated from our MD results and from Eq. (12) and the HF values of $D(q)$ are consistent with those obtained previously (Table I).

C. Collective dynamic properties

The normalized intermediate scattering function $F^N(q, t) = F(q, t)/F(q, 0)$ for liquid Ni at $T=1775$ K, $\rho=0.0792 \text{ \AA}^{-3}$ was computed for all the wave numbers of Table II except for those marked with an asterisk. Figure 6 shows the corresponding normalized dynamic structure factors $S^N(q, \omega) = S(q, \omega)/S(q)$. At the smaller q values, $S^N(q, \omega)$ presents both the central (Rayleigh) peak and a secondary (Brillouin) peak indicative of sound-wave propagation. As q increases towards $q_p = 3.0785 \text{ \AA}^{-1}$, the position of the main peak in the MD static structure factor [Fig. 1(a)], the Brillouin peak disappears and the half width at half maximum of the Rayleigh peak falls markedly (this is the ‘‘de Gennes narrowing effect,’’⁶³ which is characteristic of dense fluids and has its origin in the strong spatial correlations which exist near q_p ; Refs. 28, 32, 42, 43, and 64).

In Fig. 7 we compare the dynamic structure factor $S(q, \omega)$ for liquid Ni at $T=1875$ K, $\rho=0.078 \text{ \AA}^{-3}$, as determined from our MD simulations, with the neutron-scattering data

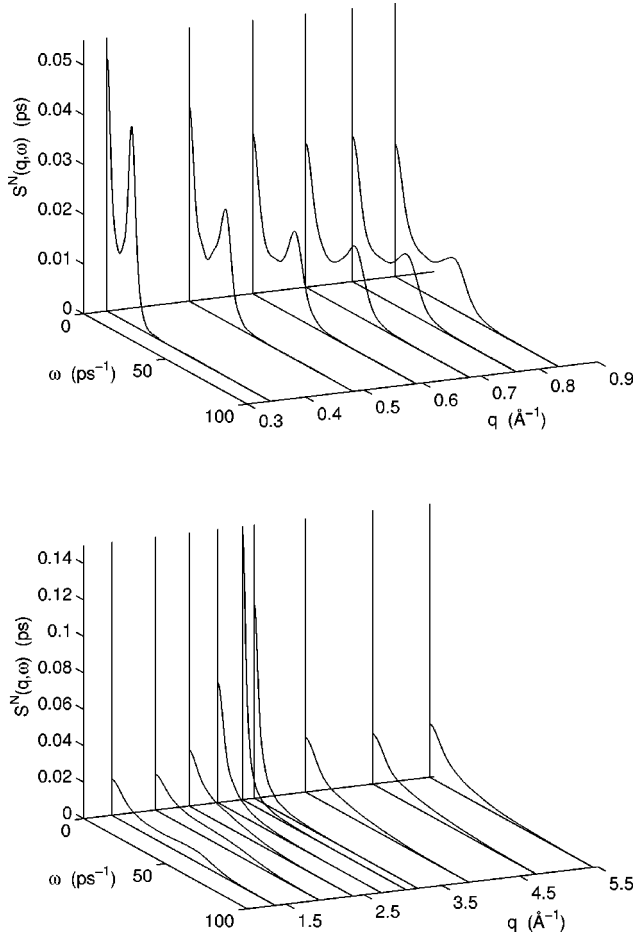


FIG. 6. Normalized dynamic structure factor $S^N(q, \omega) = S(q, \omega)/S(q)$ for liquid Ni at $T=1775$ K, $\rho=0.0792$ \AA^{-3} . Values of q are listed in Table II.

reported by Johnson *et al.*⁴⁴ for the same constant values of ω . In general, the agreement can be considered satisfactory. As in the case of $S_s(q, \omega)$, the main discrepancies occur for $\omega=0$, particularly at wave numbers close to $q_p=3.0252$ \AA^{-1} , the position of the main peak of the MD static structure factor [Fig. 1(b)]. As indicated above, these discrepancies are probably due to error in the worked-up experimental data in the $\omega=0$ region, rather than to inadequacy of the VC EAM.

For all q , the longitudinal current correlation function $C_l(q, t)$ of liquid Ni exhibits heavily damped oscillations, and $C_l(q, \omega)$ has a well-defined peak at some $\omega=\omega_{l,m}(q) > 0$. The results obtained computing $C_l(q, \omega)$ (a) as the Fourier transform of $C_l(q, t)$, and (b) from the relation $C_l(q, \omega) = \omega^2 S(q, \omega)$ (see, e.g., Ref. 51) do not show significant differences (by way of illustration, Fig. 8 shows the results for $T=1775$ K, $\rho=0.0792$ \AA^{-3} , and $q=0.832736$ \AA^{-1}).

The adiabatic speed of sound c_s was calculated for the state $T=1775$ K, $\rho=0.0792$ \AA^{-3} using the expression⁵²

$$c_s = \sqrt{\frac{1}{\rho m K_S}}, \quad (15)$$

where K_S , the adiabatic compressibility, was derived from the microcanonical MD simulations using the relation

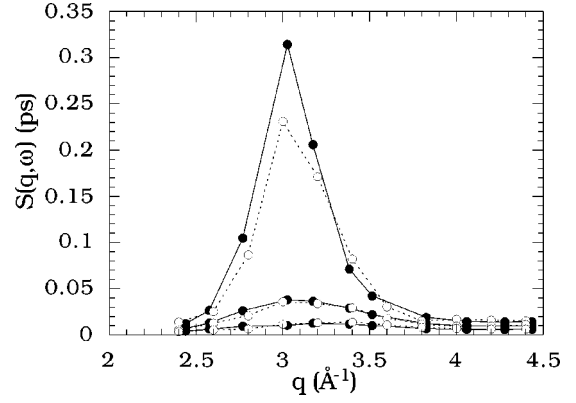


FIG. 7. Dynamic structure factor $S(q, \omega)$ of liquid Ni at $T=1875$ K, $\rho=0.078$ \AA^{-3} , for several values of ω (from top to bottom, $\omega=0, 7.60,$ and 15.19 ps^{-1}). The solid circles represent the computed results and the open circles the experimental data (Ref. 44). Lines joining points are merely visual aids.

$$\frac{1}{K_S} = \frac{N}{\rho} \left(1 - \frac{\mu}{2} \right) [\langle E_V^2 E_k^{-1} \rangle - 2 \langle E_V \rangle \langle E_V E_k^{-1} \rangle + \langle E_V \rangle^2 \langle E_k^{-1} \rangle] + \rho k T \left(1 + 2\gamma - \frac{Nk}{C_V} \right) + \frac{N}{\rho} \langle E_{VV} \rangle, \quad (16)$$

in which $\mu=3N-3$ is the number of degrees of freedom of the system (in the MD simulations the total linear momentum is fixed) and γ and C_V are the Grüneisen parameter and the heat capacity at constant volume, which are given by

$$C_V = \frac{k}{1 + (2/\mu - 1) \langle E_k \rangle \langle E_k^{-1} \rangle} \quad (17)$$

and

$$\gamma = \frac{Nk}{C_V} + \frac{N}{\rho} \left(\frac{\mu}{2} - 1 \right) [\langle E_V \rangle \langle E_k^{-1} \rangle - \langle E_V E_k^{-1} \rangle]. \quad (18)$$

In Eqs. (16) and (18), E_V and E_{VV} represent, respectively, the first and second derivatives of the energy with respect to the volume, EAM expressions for which can readily be obtained using Eq. (1). The value calculated, $c_s=42.80 \pm 0.09$ $\text{\AA} \text{ps}^{-1}$ (cf. the reported experimental values at the melting point, 40.45 $\text{\AA} \text{ps}^{-1}$ and 40.36 $\text{\AA} \text{ps}^{-1}$; Ref. 65), was used to obtain the function $\omega_s(q) = c_s q$, which is compared in Fig. 9 with the dispersion relation $\omega_{l,m}(q)$ of the longitudinal current correlation function and with the Brillouin dispersion relation $\omega_B(q)$ [i.e., the frequencies of the secondary maxima of $S(q, \omega)$, when they exist]. For small q , $\omega_{l,m}(q)$ and $\omega_B(q)$ almost coincide with each other and with $\omega_s(q)$, in compliance with the general prediction that in the hydrodynamic region $\omega_{l,m}(q) \approx \omega_B(q) \approx c_s q$.^{51,52} As in the case of other liquid metals,^{28,30,31} as q increases $\omega_{l,m}(q)$ slightly exceeds $\omega_s(q)$, which may be associated with shear relaxation effects.²⁸ The pronounced minimum of $\omega_{l,m}(q)$ near q_p has also been found in liquified noble gases,⁶⁶ liquid metals,^{28,30-32} and hard-core Yukawa fluids,⁴³ and is closely related to the de Gennes narrowing exhibited by $S(q, \omega)$.

The transverse current correlation function $C_t(q, t)$ is not directly measurable by experiment but can be computed by MD simulations. For all the q values investigated, the nor-

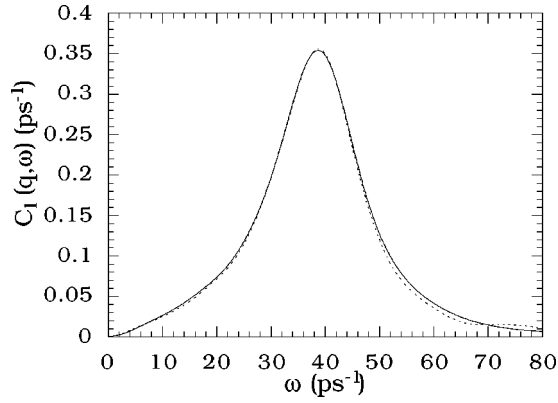


FIG. 8. The spectrum $C_1(q, \omega)$ of the longitudinal current correlation function of liquid Ni at $T=1775$ K, $\rho=0.0792 \text{ \AA}^{-3}$ for the wave number $q=0.832736 \text{ \AA}^{-1}$, as computed by calculating the Fourier transform of $C_1(q, t)$ (solid curve) and by using the relation $C_1(q, \omega) = \omega^2 S(q, \omega)$ (dashed curve).

malized function $C_i^N(q, t) = C_i(q, t)/C_i(q, 0)$ for liquid Ni at $T=1775$ K, $\rho=0.0792 \text{ \AA}^{-3}$ exhibits oscillations indicative of transverse (shear) excitations. To estimate the kinetic shear viscosity $\nu = \eta/(\rho m)$ for this state, we first estimated the generalized kinetic shear viscosity $\nu(q)$ by fitting the HF expression^{51,52}

$$C_i^N(q, t) = e^{-\nu q^2 t} \quad (19)$$

to the MD results for $C_i^N(q, t)$, and then extrapolated to $q=0$. The resulting value is in excellent agreement with the experimental value and is consistent with those derived directly from our MD simulations using the Green-Kubo and generalized Einstein expressions (Table III). The Green-Kubo and generalized Einstein values also agree well with experiment for the state $T=1875$ K, $\rho=0.078 \text{ \AA}^{-3}$ (Table III).

Figure 10 shows that all the curves $C_i^N(q, \omega)$ present a maximum at some $\omega_{i,m} > 0$. Since the dependence of $\omega_{i,m}$ on q is linear for small q (Fig. 11), a rough estimate of q_i , the critical wave number above which shear waves are supported, can be obtained (together with an estimate of c_i , the velocity of propagation of shear modes) by fitting the linear dispersion relation $\omega_{i,m} = c_i(q - q_i)$ in the low- q region of

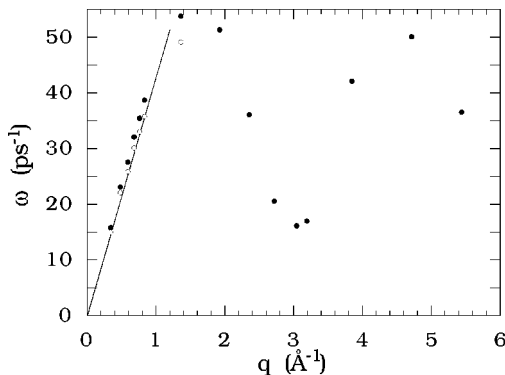


FIG. 9. Comparison of the dispersion relation $\omega_{i,m}(q)$ of the longitudinal current correlation function (solid circles), the Brillouin dispersion relation $\omega_B(q)$ (open circles) and the linear function $\omega_s(q) = c_s q$ for liquid Ni at $T=1775$ K, $\rho=0.0792 \text{ \AA}^{-3}$.

TABLE III. Values of the shear viscosity (in eV ps \AA^{-3}) for liquid Ni at $T=1775$ K, $\rho=0.0792 \text{ \AA}^{-3}$ and $T=1875$ K, $\rho=0.078 \text{ \AA}^{-3}$, as computed using the Green-Kubo (GK) and generalized Einstein (E) relations, and the respective experimental (EXPT.) data (Ref. 45). For the state $T=1775$ K, $\rho=0.0792 \text{ \AA}^{-3}$, we also show the values obtained by analyzing our $C_i(q, t)$ MD data in terms of an HF model [Eq. (19)].

	$T=1775$ K, $\rho=0.0792 \text{ \AA}^{-3}$	$T=1875$ K, $\rho=0.078 \text{ \AA}^{-3}$
GK	0.028 ± 0.002	0.022 ± 0.002
E	0.029 ± 0.002	0.024 ± 0.003
EXPT.	0.0311	0.0259
HF	0.031 ± 0.003	

Fig. 11. Although this procedure would not by itself be expected to give a very accurate estimate of q_i , the result, $q_i = 0.19 \pm 0.02 \text{ \AA}^{-1}$, agrees with the value $q_i = 0.18 \text{ \AA}^{-1}$ afforded by the expression $q_i = 2\pi/(14a)$ (which Jacucci and McDonald⁶⁷ inferred from MD results for liquid Na and K) when the nearest-neighbor distance a is set to $2.43 \pm 0.01 \text{ \AA}$, the value obtained from the radial distribution function computed using the VC EAM (the experimental value derived from x-ray measurements is $a=2.5 \text{ \AA}$; Ref. 19). Further-

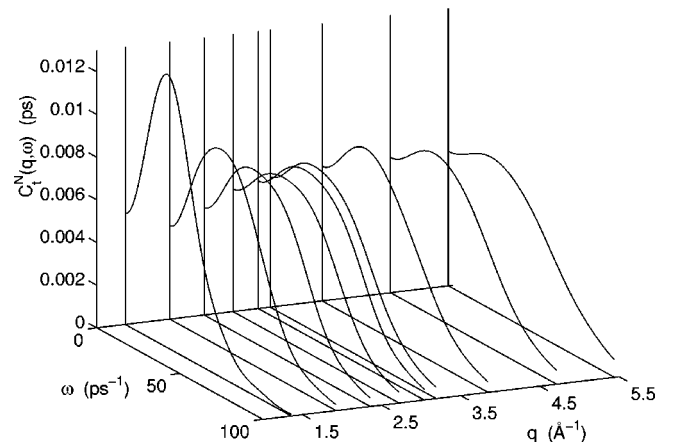
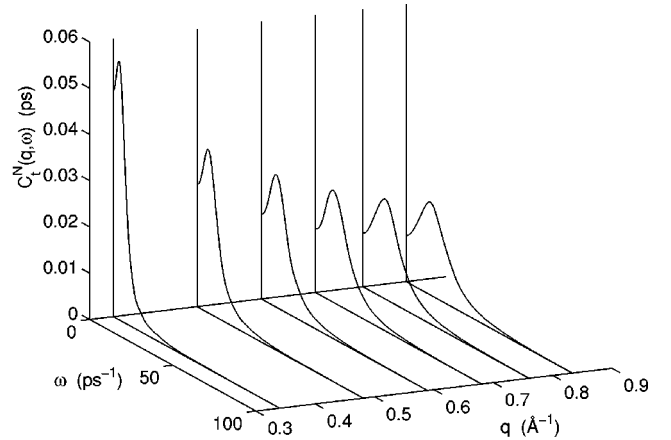


FIG. 10. The spectrum $C_i^N(q, \omega)$ of the normalized transverse current correlation function of liquid Ni in the state $T=1775$ K, $\rho=0.0792 \text{ \AA}^{-3}$. Values of q are listed in Table II.

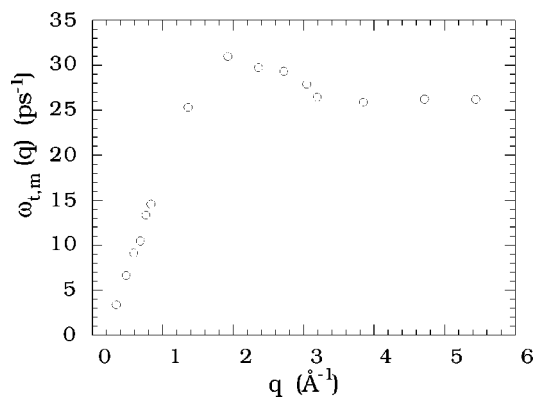


FIG. 11. Dispersion relation $\omega_{t,m}(q)$ of the transverse current correlation function for liquid Ni at $T=1775$ K, $\rho=0.0792$ Å⁻³.

more, with the same value of a , Jacucci and McDonald's⁶⁷ expression $q_l=2\pi/(1.4a)$ for the maximum wave number for longitudinal collective modes affords a value $q_l=1.8$ Å⁻¹ that is in keeping with the behavior observed in Fig. 6, which shows that longitudinal collective excitations disappear at about $q=1.923121$ Å⁻¹. Thus our results for both q_t and q_l are in keeping with the validity of Jacucci and McDonald's expressions for a nonalkali metal, and suggest that in liquid transition metals, as in liquid alkali metals,^{28,31,32,67} the q regions where sound and shear waves are supported overlap. This behavior differs from that of Lennard-Jones systems, which exhibit a q gap where neither longitudinal nor transverse modes can propagate.³⁶ As has been pointed out by Copley and Lovesey⁶⁸ and by Jacucci and McDonald,⁶⁷ these differences reflect the stronger collective character of liquid metals.

IV. SUMMARY AND CONCLUSIONS

In this work we used the VC version of the EAM in MD simulations to study the static structure and dynamic properties of liquid Ni. Like the results of other EAM approaches,^{18,23} the computed values of the static structure

factor $S(q)$ are in reasonable agreement with experimental data. The values of the dynamic structure factors $S_s(q,\omega)$ and $S(q,\omega)$ are also in quite good general agreement with the results of inelastic-neutron-scattering measurements; the main discrepancies occur at specific wave numbers when $\omega=0$, and the origin of these discrepancies may lie in the experimental data rather than in the VC EAM-based MD results. No direct experimental data on the diffusion constant D of liquid Ni are available for comparison, but the values of D obtained by using the computed mean-square displacement $\langle \Delta^2 r(t) \rangle$ and the velocity autocorrelation function $\Psi(t)$ in the Einstein and Green-Kubo equations are mutually consistent. HF, MF, and MC models fitted to our MD data give similarly consistent values of the diffusion constant. Our simulation results are also supported by the good agreement between the values of the shear viscosity calculated by various methods and available experimental data.

A priori it is not obvious whether a model potential such as the VC EAM, which uses only solid-state data and the properties of the diatomic molecule to parametrize the embedding function and pair interaction, can describe the static and dynamic properties of the liquid phase. The agreement between VC EAM predictions and available experimental results for liquid Ni is quite encouraging, and suggests that this model (and probably other EAM approaches) may also be capable of describing the dynamical properties of other liquid transition metals reasonably well. To enable this point to be verified, information derived from neutron- or light-scattering experiments on this kind of system would be welcome.

ACKNOWLEDGMENTS

We are grateful to M. W. Johnson for kindly supplying information about his experiments (Ref. 44). This work was supported by the DGICYT, Spain (Project No. PB95-0720-C02-02) and the Xunta de Galicia (Project No. XUGA20606B96). Facilities provided by the Galician Supercomputer Center (CESGA) are also acknowledged.

¹M. S. Daw and M. I. Baskes, Phys. Rev. Lett. **50**, 1285 (1983).
²M. S. Daw and M. I. Baskes, Phys. Rev. B **29**, 6443 (1984).
³M. J. Stott and E. Zaremba, Phys. Rev. B **22**, 1564 (1980).
⁴M. S. Daw, S. M. Foiles, and M. I. Baskes, Mater. Sci. Rep. **9**, 251 (1993).
⁵Ch. L. Cleveland and U. Landman, J. Chem. Phys. **94**, 7376 (1991).
⁶Z. B. Güvenç, J. Jellinek, and A. F. Voter, in *Physics and Chemistry of Finite Systems: From Clusters to Crystals*, Vol. 374 of *NATO Advanced Science Institute Series, Series C: Mathematical and Physical Sciences*, edited by P. Jena, S. N. Khanna, and B. K. Rao (Kluwer, Dordrecht, 1992), p. 411.
⁷C. Rey, L. J. Gallego, J. García-Rodeja, J. A. Alonso, and M. P. Iñiguez, Phys. Rev. B **48**, 8253 (1993).
⁸J. García-Rodeja, C. Rey, L. J. Gallego, and J. A. Alonso, Phys. Rev. B **49**, 8495 (1994).
⁹J. M. Montejano-Carrizales, M. P. Iñiguez, and J. A. Alonso, J. Cluster Sci. **5**, 287 (1994).

¹⁰J. M. Montejano-Carrizales, M. P. Iñiguez, and J. A. Alonso, Phys. Rev. B **49**, 16 649 (1994).
¹¹C. Rey, J. García-Rodeja, and L. J. Gallego, Phys. Rev. B **54**, 2942 (1996).
¹²P. R. Schwoebel, S. M. Foiles, C. L. Bisson, and G. L. Kellogg, Phys. Rev. B **40**, 10 639 (1989).
¹³A. F. Wright, M. S. Daw, and C. Y. Fong, Phys. Rev. B **42**, 9409 (1990).
¹⁴H.-V. Roy, P. Fayet, F. Patthey, W.-D. Schneider, B. Delley, and C. Massobrio, Phys. Rev. B **49**, 5611 (1994).
¹⁵M. C. Fallis, M. S. Daw, and C. Y. Fong, Phys. Rev. B **51**, 7817 (1995).
¹⁶A. F. Voter and S. P. Chen, in *Characterization of Defects in Materials*, edited by R. W. Siegel, J. R. Weertman, and R. Sinclair, MRS Symposia Proceedings No. 82 (Materials Research Society, Pittsburgh, 1987), p. 175.
¹⁷S. M. Foiles, M. I. Baskes, and M. S. Daw, Phys. Rev. B **33**, 7983 (1986).

- ¹⁸S. M. Foiles, Phys. Rev. B **32**, 3409 (1985).
- ¹⁹Y. Waseda, *The Structure of Non-Crystalline Materials* (McGraw-Hill, New York, 1980).
- ²⁰J. B. Adams and S. M. Foiles, Phys. Rev. B **41**, 3316 (1990).
- ²¹J. M. Holender, J. Phys.: Condens. Matter **2**, 1291 (1990).
- ²²J. M. Holender, Phys. Rev. B **41**, 8054 (1990).
- ²³L. M. Holzman, J. B. Adams, S. M. Foiles, and W. N. G. Hitchon, J. Mater. Res. **6**, 298 (1991).
- ²⁴R. LeSar, R. Najafabadi, and D. J. Srolovitz, J. Chem. Phys. **94**, 5090 (1991).
- ²⁵G. M. Bhuuyan, M. Silbert, and M. J. Stott, Phys. Rev. B **53**, 636 (1996).
- ²⁶S. Kambayashi and G. Kahl, Europhys. Lett. **18**, 421 (1992).
- ²⁷U. Balucani, A. Torcini, and R. Vallauri, Phys. Rev. A **46**, 2159 (1992).
- ²⁸S. Kambayashi and G. Kahl, Phys. Rev. A **46**, 3255 (1992).
- ²⁹U. Balucani, A. Torcini, and R. Vallauri, Phys. Rev. B **47**, 3011 (1993).
- ³⁰M. Canales, J. A. Padró, L. E. González, and A. Giró, J. Phys.: Condens. Matter **5**, 3095 (1993).
- ³¹M. Canales, L. E. González, and J. A. Padró, Phys. Rev. E **50**, 3656 (1994).
- ³²G. Kahl and S. Kambayashi, J. Phys.: Condens. Matter **6**, 10 897 (1994).
- ³³G. Kahl, J. Phys.: Condens. Matter **6**, 10 923 (1994).
- ³⁴A. Rahman, Phys. Rev. **136**, A405 (1964).
- ³⁵D. Levesque and L. Verlet, Phys. Rev. A **2**, 2514 (1970).
- ³⁶D. Levesque, L. Verlet, and J. Kürkijarvi, Phys. Rev. A **7**, 1690 (1973).
- ³⁷R. Vogelsang and C. Hoheisel, Mol. Phys. **53**, 1355 (1984).
- ³⁸M. Schoen, R. Vogelsang, and C. Hoheisel, Mol. Phys. **57**, 445 (1986).
- ³⁹M. Schoen and C. Hoheisel, Mol. Phys. **58**, 181 (1986).
- ⁴⁰C. Hoheisel, R. Vogelsang, and M. Schoen, J. Chem. Phys. **87**, 7195 (1987).
- ⁴¹E. Enciso, N. G. Almarza, V. del Prado, F. J. Bermejo, E. López Zapata, and M. Ujaldón, Phys. Rev. E **50**, 1336 (1994).
- ⁴²W. E. Alley, B. J. Alder, and S. Yip, Phys. Rev. A **27**, 3174 (1983).
- ⁴³M. M. G. Alemany, C. Rey, and L. J. Gallego, J. Chem. Phys. **105**, 8250 (1996).
- ⁴⁴M. W. Johnson, B. McCoy, N. H. March, and D. I. Page, Phys. Chem. Liq. **6**, 243 (1977).
- ⁴⁵M. Shimoji and T. Itami, *Atomic Transport in Liquid Metals* (Trans Tech Publications, Aedermannsdorf, Switzerland, 1986).
- ⁴⁶M. W. Johnson, N. H. March, B. McCoy, S. K. Mitra, D. I. Page, and R. C. Perrin, Philos. Mag. **33**, 203 (1976).
- ⁴⁷J. H. Rose, J. R. Smith, F. Guinea, and J. Ferrante, Phys. Rev. B **29**, 2963 (1984).
- ⁴⁸R. Hultgren, P. D. Desai, D. T. Hawkins, M. Gleiser, K. K. Kelley, and D. D. Wagman, *Selected Values of the Thermodynamic Properties of the Elements* (American Society for Metals, Metals Park, OH, 1973).
- ⁴⁹S. Nosé, Mol. Phys. **52**, 255 (1984).
- ⁵⁰M. P. Allen and D. J. Tildesley, *Computer Simulation of Liquids* (Oxford University Press, Oxford, 1990).
- ⁵¹J. P. Hansen and I. R. McDonald, *Theory of Simple Liquids* (Academic, London, 1986).
- ⁵²J. P. Boon and S. Yip, *Molecular Hydrodynamics* (McGraw-Hill, New York, 1980).
- ⁵³M. J. Huijben and W. van der Lugt, Acta Crystallogr., Sect. A: Cryst. Phys., Diffr., Theor. Gen. Crystallogr. **35**, 431 (1979).
- ⁵⁴H. Olbrich, H. Ruppertsberg, and S. Steeb, Z. Naturforsch. A **38**, 1328 (1983).
- ⁵⁵J. R. D. Copley and S. W. Lovesey, in *Liquid Metals 1976*, edited by R. Evans and D. A. Greenwood IOP Conf. Proc. No. 30 (Institute of Physics, London, 1977), p. 575.
- ⁵⁶W. Martin, W. Freyland, P. Lamparter, and S. Steeb, Phys. Chem. Liq. **10**, 49 (1980).
- ⁵⁷Figure 4.1 of Ref. 44 is misprinted: the crosses represent theoretical values and the curves experimental values. This has been confirmed by M. W. Johnson (private communication).
- ⁵⁸This possible explanation of the origin of the discrepancies between our MD results and their experiments when $\omega=0$ has been confirmed by M. W. Johnson (private communication).
- ⁵⁹L. E. González, D. J. González, and M. Canales, Z. Phys. B **100**, 601 (1996).
- ⁶⁰L. E. González, D. J. González, M. Silbert, and J. A. Alonso, J. Phys.: Condens. Matter **5**, 4283 (1993).
- ⁶¹I. M. de Schepper and M. H. Ernst, Physica A **98**, 189 (1979).
- ⁶²P. Verkerk, Nuovo Cimento D **12**, 441 (1990).
- ⁶³P. G. de Gennes, Physica (Amsterdam) **25**, 825 (1959).
- ⁶⁴U. Balucani and R. Vallauri, Phys. Rev. A **40**, 2796 (1989).
- ⁶⁵T. Iida and R. I. L. Guthrie, *The Physical Properties of Liquid Metals* (Clarendon, Oxford, 1988).
- ⁶⁶N. K. Ailawadi, A. Rahman, and R. Zwanzig, Phys. Rev. A **4**, 1616 (1971).
- ⁶⁷G. Jacucci and I. R. McDonald, Mol. Phys. **39**, 515 (1980).
- ⁶⁸J. R. D. Copley and S. W. Lovesey, Rep. Prog. Phys. **38**, 461 (1975).